# Reconstruction of sampled complex processes with timing jitter

Bernard Lacaze, Corinne Mailhes

# Reconstruction of sampled complex processes with timing jitter

Bernard Lacaze
IRIT / TéSA, 2 rue Camichel, BP7122
31071 Toulouse Cédex 7, France
Bernard.Lacaze@tesa.prd.fr

Corinne Mailhes
ENSEEIHT / IRIT / TéSA, 2 rue Camichel, BP7122
31071 Toulouse Cédex 7, France
Corinne.Mailhes@tesa.prd.fr

**Abstract**

This paper studies the effec ts of timing jitter onc omplec proc esses, whether the samplingc ondition is verified or not. The problem of recovering ac ontinuous-time process from observations subjected to jitter isc onsidered. A solution in terms of linear filtering of sampled real and imaginary parts is derived. Simulation ecamples are given to demonstrate the application of the proposed scheme.

*Key words ssd phrsses* : sampling,c omplec proc esses, timing jitter, linear minimum mean square reconstruction

## 1 Introduction

The well-known sampling theorem states that a continuous-time band-limited process can be recovered from a set of samples in the case of periodic sampling if the sampling frequency is twice the spectral band limit of the process. Indeed, when the sampling theorem is verified, the reconstruction of the original continuous-time process can be achieved with a zero mean square error (MSE) by a linear interpolation of the samples. This interpolator is referred to as the Shannon interpolator. When the hypotheses of the sampling theorem are not fulfilled, the linear

reconstruction with a zero MSE is not possible. However, the linear minimum mean square estimator (LMMSE) can be derived.

In the case of complex processes, it has been shown that a lower MSE can often be achieved by considering a linear combination of the observed real part and imaginary part samples rather than a linear combination of the complex samples [1], [2]. However, the results of [1], [2] have been obtained under uniform sampling assumption.

The problem of jitter in sampling has received an increasing attention in recent years because as sampling rates become higher, the effect of jitter on system performance can no longer be neglected. Early papers [3], [4] derived the expression of the discrete sampled sequence spectrum as a function of the continuous signal spectrum. More recent papers study the effect of timing jitter in equivalent-time sampling systems [5], [6] and proposed two amplitude estimators based on a mean estimator or a Markov estimator. The effect of timing jitter in equispaced sampling wattmeters is studied in [7], assuming that timing jitter introduces random fluctuations in the sampling instants of both voltage and current channels. In order to estimate the jitter variance in high frequency sampling scopes, a maximum likelihood estimator is proposed and compared to the least squares estimator [8]. An original method based on the bispectrum is derived in [9], [10] to detect sampling jitter and estimate its variance. In these papers, the reconstruction of the original signal is achieved by assuming that multiple samples are taken at each nominal sample time, allowing to propose estimators based on mean computation, for example. The problem of signal reconstruction in the presence of jitter, using one set of samples (i.e., one sample at each nominal sample time) has been studied in [11]: three methods are derived from optimization techniques to reconstruct a bandlimited discrete-time signal from an irregular set of samples at unknown locations. It is interesting to note that in this case, the continuous-time reconstruction is not addressed and a spectral bandlimitedness hypothesis is necessary to apply the methods proposed in [11].

The present paper addresses the problem of recovering a continuous-time complex process from sampled observations subjected to timing jitter, without any hypothesis on the signal spectral band.

The main results of [1], [2] are recalled in Section 2 and the formulation of timing jitter problem is given. Section 3 first derives the solution to a general problem: how can we reconstruct one random process, based

on the observation of two others random processes, correlated to the one we are willing to reconstruct. Then, applied to the precise context of the paper, the LMMSE expression is given, allowing to reconstruct a complex random process based on the observations of its real and imaginary sampled parts in the presence of timing jitter. Section 4 gives some examples and simulations highlight how the results of the Section 3 can be applied. Conclusions are reported in Section 5. Appendices are given in order to detail some theoretical developments necessary to derive the results of Section 3.

# 2 Problem formulation

## 2.1 Uniform sampling

Let $\mathbf{Z} = \{Z(t), t \in \mathbb{R}\}$ be a complex random process whose real and imaginary parts are denoted as $\mathbf{X} = \{X(t), t \in \mathbb{R}\}$ and $\mathbf{Y} = \{Y(t), t \in \mathbb{R}\}$

$$Z(t) = X(t) + iY(t). \tag{1}$$

The random process $\mathbf{Z}$ is a zero mean stationary process whose Power Spectral Density (PSD) $s_Z(\omega)$ is defined by

$$K_Z(\tau) = E\left[Z(t) Z^*(t-\tau)\right] = \int_{\mathbb{R}} s_Z(\omega) e^{i\omega\tau} d\omega \tag{2}$$

where $E[.]$ denotes the mathematical expectation, the superscript $*$ holds for complex conjugate and $K_Z(\tau)$ denotes the random process autocorrelation function. The PSDs $s_X(\omega)$ and $s_Y(\omega)$ of $\mathbf{X}$ and $\mathbf{Y}$ are defined in the same way, from the autocorrelation functions $K_X(\tau)$ and $K_Y(\tau)$. Moreover, $X(t)$ and $Y(t)$ are assumed to be stationary correlated and the interspectrum $s_{XY}(\omega)$ is defined by

$$K_{XY}(\tau) = E\left[X(t) Y(t-\tau)\right] = \int_{\mathbb{R}} s_{XY}(\omega) e^{i\omega\tau} d\omega. \tag{3}$$

Straightforward computations allow to express $s_Z(\omega)$ as follows

$$s_Z(\omega) = s_X(\omega) + s_Y(\omega) - is_{XY}(\omega) + is_{XY}^*(\omega). \tag{4}$$

The random process $\mathbf{Z}$ is sampled at time instants $t = n \in \mathbb{Z}$, with a unit sampling period. The classical sampling theory studies linear reconstruction of the continuous random process $\mathbf{Z}$ based on the observation

of its samples [12]. For example, in the case of a random process with a limited spectral band of $[-\pi, +\pi]$, the reconstruction is exact (i.e., with a zero MSE) using the following formula:

$$Z(t) = \sum_{k=-\infty}^{+\infty} \frac{\sin(\pi(t-k))}{\pi(t-k)} Z(k). \tag{5}$$

More generally, without any hypothesis on the spectral bandwidth, the uniform sampling of the random process $\mathbf{Z}$ allows to derive the LMMSE of $Z(t)$ from the sampled process $\mathbf{Z}_s = \{Z(n), n \in \mathbb{Z}\}$ [13], [14]. This LMMSE is a linear combination of the observed samples and can be written in a general form:

$$\widehat{Z_1}(t) = \lim_{n \to +\infty} \sum_{k=-n}^{n} a_{kn}(t) Z(k) \tag{6}$$

where the limit is defined in the mean square sense. This linear reconstruction is optimal in the sense that the coefficients $a_{kn}(t)$ are calculated in order to minimize the MSE

$$\sigma_1^2 = E\left[\left|Z(t) - \widehat{Z_1}(t)\right|^2\right] \tag{7}$$

where $\widehat{Z_1}(t)$ is a linear interpolator defined in (6).

Of course, the knowledge of the complex sampled process $\mathbf{Z}_s$ is equivalent to the knowledge of its sampled real and imaginary parts, $\mathbf{X}_s = \{X(n), n \in \mathbb{Z}\}$ and $\mathbf{Y}_s = \{Y(n), n \in \mathbb{Z}\}$. However, it has been shown [1], [2] that a lower MSE can be possibly obtained by considering a linear interpolator of the form

$$\widehat{Z_2}(t) = \lim_{n \to +\infty} \sum_{k=-n}^{n} b_{kn}(t) X(k) + c_{kn}(t) Y(k). \tag{8}$$

## 2.2 Non uniform sampling

When sampling errors occurred during the sampling process, the sampled complex observations can be written

$$\breve{Z}(n) = Z(n - A(n)) \tag{9}$$

where timing jitter is modeled by a random sequence $\mathbf{A}_s = \{A(n), n \in \mathbb{Z}\}$ independent of $\mathbf{Z}$. The jitter is assumed to be stationary in the sense that the two following characteristic functions [15] are independent of $n$:

$$\begin{aligned} \Psi(\omega) &= E\left[e^{i\omega A(n)}\right] \\ \Phi(m,\omega) &= E\left[e^{i\omega(A(n)-A(n-m))}\right]. \end{aligned} \tag{10}$$

This paper addresses the problem of finding the LMMSE $\widehat{Z}(t)$ of $Z(t)$ from the observations $\breve{\mathbf{Z}}_s = \left\{\breve{Z}(n), n \in \mathbb{Z}\right\}$. Note that the jitter sequence $\mathbf{A}_s$ is not observed and is only known by its characteristic functions given in (10). The reconstruction of $Z(t)$ from $\breve{\mathbf{Z}}_s$ can be achieved, as in the uniform sampling case, by the following linear interpolation:

$$\widehat{Z_3}(t) = \lim_{n\to+\infty} \sum_{k=-n}^{n} a_{kn}(t)\, \breve{Z}(k) \tag{11}$$

where the interpolation coefficients $a_{kn}(t)$ depend on the statistical properties of the jitter sequence $\mathbf{A}_s$. Such problem has been addressed by Balakrishnan in [3]. Related studies can also be found in [16] and [17].

The main contribution of this paper is the reconstruction of $Z(t)$ by using the following linear interpolator

$$\widehat{Z}(t) = \lim_{n\to+\infty} \sum_{k=-n}^{n} \left(b_{kn}(t)\, \breve{X}(k) + c_{kn}(t)\, \breve{Y}(k)\right) \tag{12}$$

where $\breve{X}(k) = X(k - A(k))$ and $\breve{Y}(k) = Y(k - A(k))$ are the real and imaginary parts of the observed sampled process $\breve{\mathbf{Z}}_s = \left\{\breve{Z}(k), k \in \mathbb{Z}\right\}$. The determination of the interpolation coefficients $b_{kn}(t)$ and $c_{kn}(t)$ is related to a more general problem addressed in the next section.

# 3 LMMSE derivation

The first part of this section studies the recovery of a random sequence $\mathbf{W}_s = \{W(n), n \in \mathbb{Z}\}$ from the observation of two other sequences $\mathbf{U}_s = \{U(n), n \in \mathbb{Z}\}$ and $\mathbf{V}_s = \{V(n), n \in \mathbb{Z}\}$, both correlated with $\mathbf{W}_s$. The determination of the LMMSE defined in (12) is studied in the second part of this section.

### 3.1 A general problem

The three random sequences $\mathbf{U}_s$, $\mathbf{V}_s$ and $\mathbf{W}_s$ are assumed to be stationary, with stationary intercorrelations. The autocorrelation functions of the three random sequences allow to define their respective PSDs $\widetilde{s}_U(\omega), \widetilde{s}_V(\omega)$ and $\widetilde{s}_W(\omega)$, defined on $[-\pi, +\pi]$, from the Herglotz lemma [18]. For sake of clarity, only one spectrum definition is given: for example, $\widetilde{s}_U(\omega)$ is defined by

$$K_U(m) = E[U(n)\, U^*(n-m)] = \int_{-\pi}^{+\pi} \widetilde{s}_U(\omega)\, e^{i\omega m} d\omega \quad (m,n) \in \mathbb{Z}^2. \tag{13}$$

The stationary intercorrelations of the three random sequences $\mathbf{U}_s$, $\mathbf{V}_s$ and $\mathbf{W}_s$ allow to define the interspectra of these sequences. For example, $\widetilde{s}_{UV}(\omega)$ is defined by

$$K_{UV}(m) = E[U(n)\, V^*(n-m)] = \int_{-\pi}^{+\pi} \widetilde{s}_{UV}(\omega)\, e^{i\omega m} d\omega \quad (m,n) \in \mathbb{Z}^2. \tag{14}$$

Appendix B shows that the LMMSE of $W(n)$ (denoted as $\widehat{W}(n)$) from the observation of $\{U(n), n \in \mathbb{Z}\}$ and $\{V(n), n \in \mathbb{Z}\}$ can be viewed as the sum of the outputs of two time-invariant linear filters driven respectively by $U(n)$ and $V(n)$, as illustrated on Fig. 1.

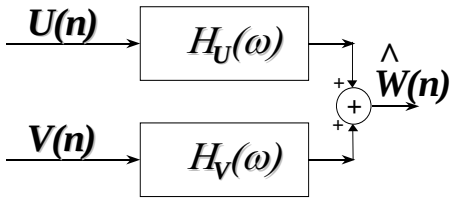


Figure 1: Reconstruction of $W(n)$ from the observation of $U(n)$ and $V(n)$.

Straightforward computations (see Appendix B) allow to determine

the frequency responses of these filters, denoted as $H_U(\omega)$ and $H_V(\omega)$

$$\begin{aligned} H_U(\omega) &= \frac{\widetilde{s}_{WU}(\omega)\,\widetilde{s}_V(\omega) - \widetilde{s}_{WV}(\omega)\,\widetilde{s}_{VU}(\omega)}{\widetilde{s}_U(\omega)\,\widetilde{s}_V(\omega) - |\widetilde{s}_{UV}(\omega)|^2} \\ H_V(\omega) &= \frac{\widetilde{s}_{WV}(\omega)\,\widetilde{s}_U(\omega) - \widetilde{s}_{WU}(\omega)\,\widetilde{s}_{UV}(\omega)}{\widetilde{s}_U(\omega)\,\widetilde{s}_V(\omega) - |\widetilde{s}_{UV}(\omega)|^2}. \end{aligned} \tag{15}$$

Moreover, the MSE $\sigma_W^2$ between the original sequence $W(n)$ and its reconstruction $\widehat{W}(n)$ can be expressed as follows:

$$\begin{aligned} \sigma_W^2 &= E\left[\left|W(n) - \widehat{W}(n)\right|^2\right] \\ &= \int_{-\pi}^{+\pi} \left( \widetilde{s}_W(\omega) - \frac{|\widetilde{s}_{WU}(\omega)|^2}{\widetilde{s}_U(\omega)} \right. \\ &\qquad \left. - \frac{|\widetilde{s}_{WV}(\omega)\,\widetilde{s}_U(\omega) - \widetilde{s}_{WU}(\omega)\,\widetilde{s}_{UV}(\omega)|^2}{\widetilde{s}_U(\omega)\left(\widetilde{s}_U(\omega)\,\widetilde{s}_V(\omega) - |\widetilde{s}_{UV}(\omega)|^2\right)} \right) d\omega. \end{aligned} \tag{16}$$

### 3.2 Reconstruction of a complex random process sampled with timing jitter

This section applies the results obtained in the previous sub-section 3.1 to the following particular case

$$\begin{aligned} W(n) &= Z(t+n) = X(t+n) + iY(t+n) \\ U(n) &= X(n - A(n)) = \breve{X}(n) \text{ and } V(n) = Y(n - A(n)) = \breve{Y}(n). \end{aligned} \tag{17}$$

Appendix C shows that the assumptions necessary to express $\widehat{W}(n) = \widehat{Z}(t+n)$ as in Fig. 1 are satisfied for any fixed $t$. As a consequence, the reconstruction of $W(n) = Z(t+n)$ can be obtained by means of two time-varying filters as illustrated on Fig. 2. Computations detailed in the Appendix C allow to derive the expressions of the different spectra and interspectra (see (64) and (66) in the Appendix C) which are necessary to compute the expressions of the two linear filters $H_U(t,\omega)$ and $H_V(t,\omega)$ given by (15). The interpolation coefficients $b_k(t)$ and $c_k(t)$ of (12) are the impulse responses of these two filters

$$\begin{aligned} b_k(t) &= \frac{1}{2\pi}\int_{-\pi}^{+\pi} H_U(t,\omega)\, e^{i\omega k} d\omega \\ c_k(t) &= \frac{1}{2\pi}\int_{-\pi}^{+\pi} H_V(t,\omega)\, e^{i\omega k} d\omega. \end{aligned} \tag{18}$$

Moreover, the MSE of reconstruction can be derived by (16), since the required spectra and interspectra have been defined in (64) and (66).

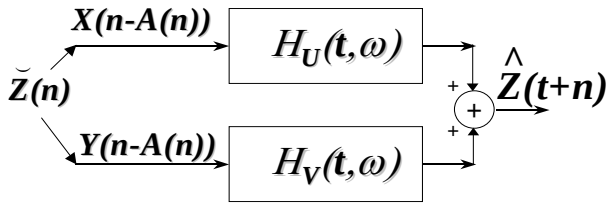


Figure 2: Reconstruction of $Z(t)$.

# 4 Simulation results

## 4.1 Example of uncorrelated real and imaginary parts

This first example takes into consideration a complex random process with uncorrelated real and imaginary parts $\mathbf{X}$ and $\mathbf{Y}$ ($s_{XY}(\omega) = 0$) with uniform DSPs on $[-\pi, \pi]$

$$\begin{cases} s_X(\omega) & = s_Y(\omega) = \frac{1}{2\pi} \quad \text{for} \quad \omega \in [-\pi, \pi] \\ s_X(\omega) & = s_Y(\omega) = 0 \quad \text{elsewhere.} \end{cases} \tag{19}$$

The jitter sequence $\mathbf{A}_s = \{A(n), n \in \mathbb{Z}\}$ is assumed to be independent, identically distributed (i.i.d.) with uniform distribution on $[-a, +a]$

$$\begin{cases} \Psi(\omega) & = \frac{\sin(a\omega)}{a\omega} \\ \Phi(m,\omega) & = \left(\frac{\sin(a\omega)}{a\omega}\right)^2 \quad m \neq 0 \qquad \text{and} \qquad \Phi(0,\omega) = 1. \end{cases} \tag{20}$$

In this example, $\breve{X}(n)$ and $\breve{Y}(n)$ have the same properties. Consequently, it is not surprising that (based on the results of Appendix B and Appendix C) the reconstruction filters satisfy $H_V(\omega) = iH_U(\omega)$. Moreover, based on the results of Appendix B and Appendix C, we obtain

$$H_U(\omega) = e^{i\omega t} \frac{a\omega \sin(a\omega)}{\sin^2(a\omega) + (a\omega)^2 q_a} \tag{21}$$

where

$$q_a = 1 - \frac{1}{2\pi} \int_{-\pi}^{+\pi} \left(\frac{\sin(ax)}{ax}\right)^2 dx. \tag{22}$$

Consequently, the LMMSE defined in (12) is of the form

$$\widehat{Z}(t) = \sum_{k\in\mathbb{Z}} b_k(t) \left( \breve{X}(k) + i\breve{Y}(k) \right). \tag{23}$$

The interpolation coefficients $b_k(t)$ cannot be expressed in closed form for this example. However, a standard FIR implementation can be conducted (see [19] for more details on RIF implementation). Figure 3 shows examples of these coefficients for different values of the jitter parameter $a$ and reconstruction time instant $t$ (due to a symmetry property of these coefficients, only time instants from 0 to 0.5 are considered).

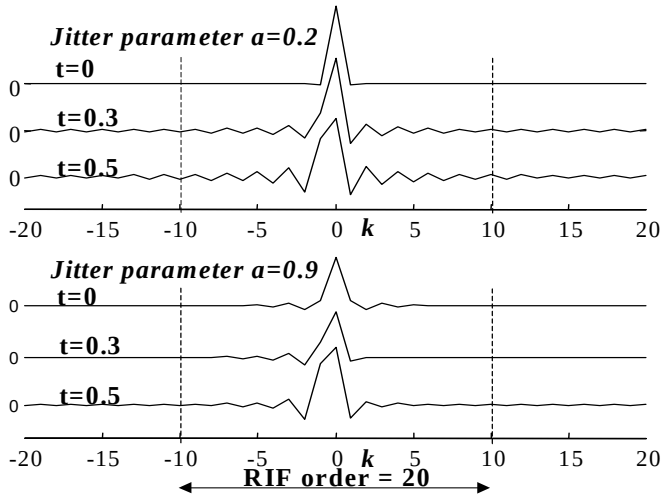


Figure 3: Reconstruction coefficients for different values of jitter parameter $a$ and time instant $t$.

The expression of the MSE $\sigma_Z^2$ given by (16) can also be derived

$$\sigma_Z^2 = 2 - \frac{1}{\pi} \int_{-\pi}^{+\pi} \frac{\sin^2(a\omega)}{\sin^2(a\omega) + (a\omega)^2 q_a} d\omega. \tag{24}$$

It is interesting to compare this proposed LMMSE to the standard interpolator of Shannon. Note that the Shannon interpolator can be retrieved from (21) by setting $a = 0$ (absence of jitter). The reconstruction Shannon filters and the corresponding interpolation coefficients are of the

form

$$H_U(\omega) = e^{i\omega t}, \qquad H_V(\omega) = ie^{i\omega t}, \qquad c_k(t) = \frac{\sin(\pi(t+k))}{\pi(t+k)}. \quad (25)$$

The main interest of the Shannon interpolator is that its expression is not related to the random process which has been sampled. However, this interpolator does not take into consideration the timing jitter effect. Under appropriate conditions, the Shannon interpolator yields a zero MSE. However, in the presence of jitter, these conditions are not satisfied and the reconstructed random process $\widehat{\mathbf{Z}}_{Shan} = \left\{\widehat{Z}_{Shan}(t), t \in \mathbb{R}\right\}$ issued from the Shannon interpolator is such that

$$E\left[\left|\widehat{Z}_{Shan}(n) - Z(n)\right|^2\right] = E\left[\left|\breve{Z}(n) - Z(n)\right|^2\right] = \sigma^2_{jit}. \quad (26)$$

In other words, the reconstruction of $Z(t)$ by the Shannon interpolator is not better than the random variable $\breve{Z}(n)$ itself in terms of MSE. By taking into consideration (19) and (20), the expression of this last MSE can be derived as a function of the jitter parameter $a$

$$\sigma^2_{jit} = 4 - \frac{2}{a}\int_{-a}^{+a} \frac{\sin(\pi\theta)}{\pi\theta} d\theta. \quad (27)$$

The comparison between the proposed LMMSE and the Shannon interpolator in terms of MSE is illustrated in Fig. 4 as a function of the jitter parameter $a$. Note that the MSEs are normalized. These simulations show that the theoretical expressions derived in this paper are in good agreement with the estimated MSEs. Moreover, the Shannon interpolator becomes rapidly inefficient (in terms of reconstruction of $Z(t)$) when parameter $a$ increases. Figure 5 shows an example of a complex process and its reconstruction in the case of a jitter parameter $a = 0.2$. In this case, the reconstruction error is small as expected (see Fig. 4). Figure 6 illustrates the case of a reconstruction in the presence of jitter with parameter $a = 0.9$. The estimated normalized MSE equals 57%, which shows the limitation of the LMMSE.

### 4.2 Example of correlated real and imaginary parts, out of sampling condition.

The second example developed in this section studies a complex random process that does not satisfy the Nyquist conditions, with correlated real

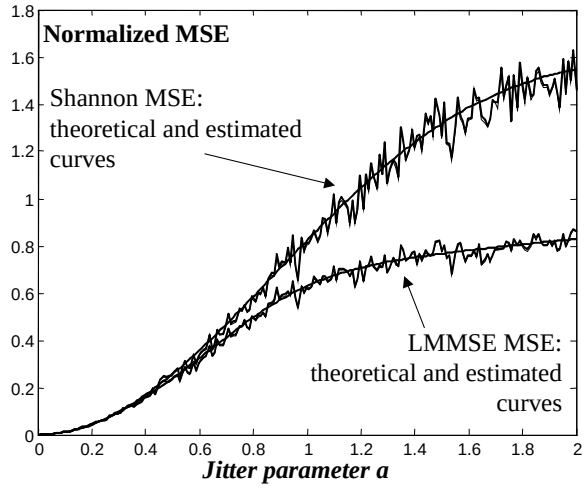


Figure 4: Normalized MSE v.s. jitter parameter.

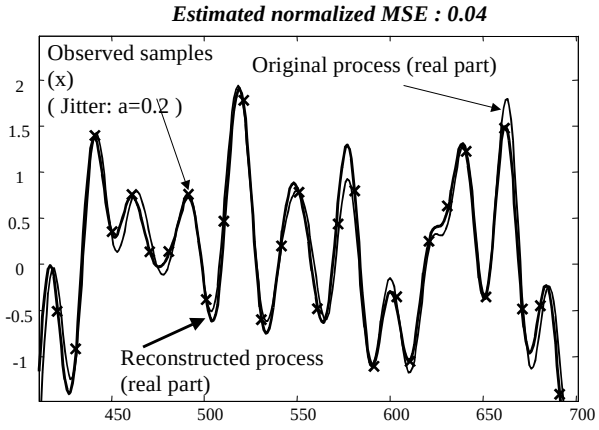


Figure 5: Example of a complex random process (only the real part is represented) and its reconstruction in the case of jitter (parameter $a = 0.2$).

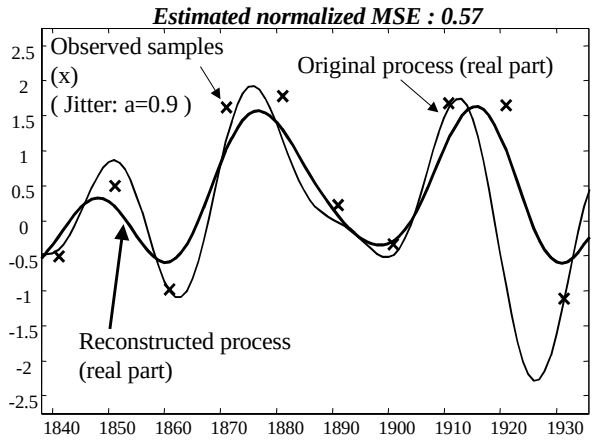


Figure 6: Example of a complex random process (only the real part is represented) and its reconstruction in the case of jitter (parameter $a = 0.9$).

and imaginary parts. More precisely, the complex random process $\mathbf{Z}$ is such that its real and imaginary part are linked by the following relation:

$$\mathbf{Y} = 2\mathcal{H}(\mathbf{X}) \tag{28}$$

where $\mathcal{H}(.)$ denotes the Hilbert filter. The PSD of $\mathbf{X}$ is assumed to be defined as

$$s_X(\omega) = \frac{1}{4\pi} \quad \text{for } \omega \in [-2\pi, +2\pi] \qquad \text{and} \qquad s_X(\omega) = 0 \quad \text{elsewhere.}$$

In this case, (28) yields

$$\begin{array}{llll} s_Y(\omega) & = \frac{1}{\pi} \text{ for } \omega \in [-2\pi, +2\pi] & s_Y(\omega) & = 0 \text{ elsewhere} \\ s_{XY}(\omega) & = \frac{i}{2\pi}\text{sign}(\omega) \text{ for } \omega \in [-2\pi, +2\pi] & s_{XY}(\omega) & = 0 \text{ elsewhere} \end{array} \tag{29}$$

where sign($\omega$) is the signum function (equal to +1 if its argument is non-negative and -1 if its argument is negative). The jitter sequence $\mathbf{A}_s = \{A(n), n \in \mathbb{Z}\}$ is assumed to be independent, identically distributed (i.i.d.) with discrete uniform distribution on $\{-\varepsilon, \varepsilon\}$ ($P[A(n) = \varepsilon] = P[A(n) = -\varepsilon] = 0.5$). The corresponding characteristic functions of the

jitter are defined as

$$\begin{cases} \Psi(\omega) & = \cos(\varepsilon\omega) \\ \Phi(m,\omega) & = \cos^2(\varepsilon\omega) \quad m \neq 0 \qquad \text{and} \qquad \Phi(0,\omega) = 1. \end{cases} \tag{30}$$

Appendix B and Appendix C show that the reconstruction filters of Fig. 2 have the following transfer functions

$$\begin{aligned} H_U(\omega) &= e^{i\omega t}\left[\begin{array}{c}(1+2\text{sign}(\omega))\,H_\varepsilon(\varepsilon\omega) \\ +(1-2\text{sign}(\omega))\,e^{-i2\pi\text{sign}(\omega)t}H_\varepsilon(\varepsilon\omega-2\pi\varepsilon\text{sign}(\omega))\end{array}\right] \\ H_V(\omega) &= \frac{i}{2}e^{i\omega t}\left[\begin{array}{c}(2+\text{sign}(\omega))\,H_\varepsilon(\varepsilon\omega) \\ +(2-\text{sign}(\omega))\,e^{-i2\pi\text{sign}(\omega)t}H_\varepsilon(\varepsilon\omega-2\pi\varepsilon\text{sign}(\omega))\end{array}\right] \end{aligned} \tag{31}$$

where

$$H_\varepsilon(\omega) = \frac{\cos\omega}{1-\frac{\sin(4\pi\varepsilon)}{4\pi\varepsilon}+2\cos^2\omega}. \tag{32}$$

Figure 7 shows the corresponding impulse responses for a jitter parameter $\varepsilon = 0.1$. As in the previous example, the time support of these impulse responses can be approximated by 20 coefficients (in our simulations, this is true for any value of $\varepsilon$). As a consequence, the reconstruction filters can be implemented as FIR filters with small order.

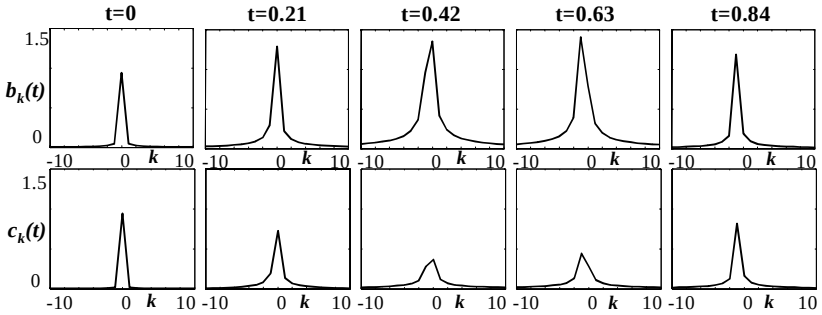


Figure 7: Interpolation coefficients $|b_k(t)|$ and $|c_k(t)|$ for different time instants $t$ ($\varepsilon = 0.1$).

The MSE defined in (16) can be derived

$$\sigma_Z^2 = 5 - \int_{-\pi}^{+\pi} \frac{N(\omega)}{D(\omega)} d\omega \tag{33}$$

where

$$\begin{aligned} N(\omega) &= (4S(\omega)+5)\cos^2(\varepsilon\omega) + (-4S(\omega)+5)\cos^2(\varepsilon\omega - 2\pi\varepsilon S(\omega)) \\ &\quad +20\cos^2(\varepsilon\omega)\cos^2(\varepsilon\omega - 2\pi\varepsilon S(\omega)) \\ D(\omega) &= 2\pi\left(1-\operatorname{sinc}(4\pi\varepsilon)+2\cos^2(\varepsilon\omega)\right) \\ &\quad \left(1-\operatorname{sinc}(4\pi\varepsilon)+2\cos^2(\varepsilon\omega - 2\pi\varepsilon S(\omega))\right) \end{aligned} \tag{34}$$

It is important to note that the MSE does not depend on the time instant $t$. Note also that in the absence of jitter, the exact reconstruction of $Z(t)$ based on the observation of the sampling sequence $\mathbf{Z}_s = \{Z(n), n \in \mathbb{Z}\}$ is not possible because the spectral bandwidth of $Z(t)$ is $4\pi$. This exact reconstruction is only allowed by considering the real and imaginary parts of the sampled process separately, as shown in [1], and introducing a linear interpolator of the form of (8). In this case, by setting $\varepsilon = 0$ in (31), the interpolation coefficients can be expressed as

$$\begin{aligned} b_k(t) &= \frac{-i}{4\pi(t+k)}\left(-4+3e^{i2\pi t}+e^{-i2\pi t}\right) \\ c_k(t) &= \frac{1}{8\pi(t+k)}\left(-2+3e^{i2\pi t}-e^{-i2\pi t}\right). \end{aligned} \tag{35}$$

Consequently, in the presence of jitter, the MSE $\sigma_Z^2$ will tend to zero as $\varepsilon$ decreases. Figure 8 illustrates this behavior, as a function of the jitter parameter value $\varepsilon$. Figure 8 also shows that the theoretical and estimated MSEs for the LMMSE are in good agreement. Figure 9 compares the MSEs of the LMMSE and the linear interpolator derived without considering jitter effects (the expression of the interpolator coefficients are given in (35)). Obviously, the LMMSE outperforms the other interpolator for large values of $\varepsilon$. Figure 10 shows an example of a complex random process and its reconstruction for $\varepsilon = 0.1$.

# 5 Conclusions

This paper studies the reconstruction of random complex processes sampled periodically with timing jitter. It is shown that the recovery of the original continuous-time process can be considered by using a linear interpolator with different interpolation coefficients relative to the real and imaginary parts of the observed sampled process. The theoretical

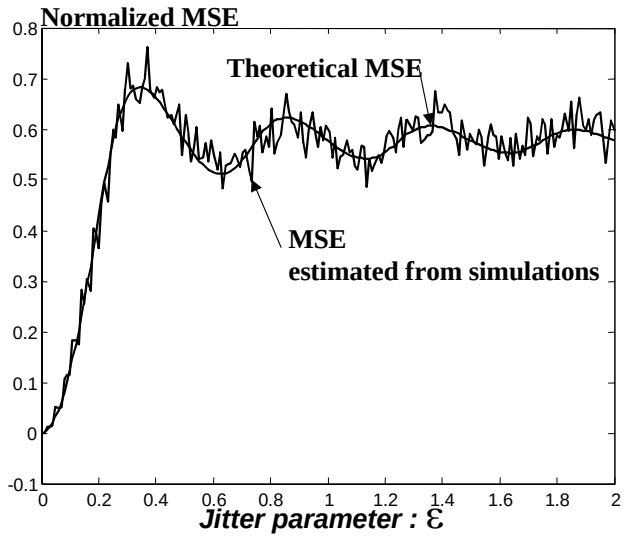


Figure 8: Theoretical and estimated MSEs as a function of the jitter parameter $\varepsilon$.

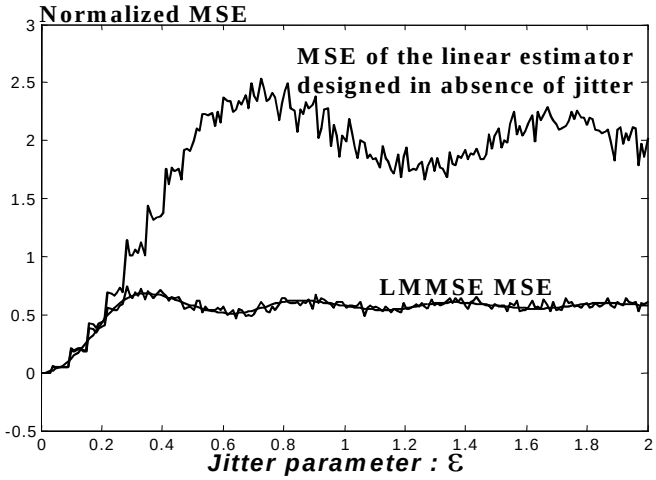


Figure 9: MSEs for the LMMSE and the linear estimator designed in absence of jitter, as a function of the jitter parameter $\varepsilon$.

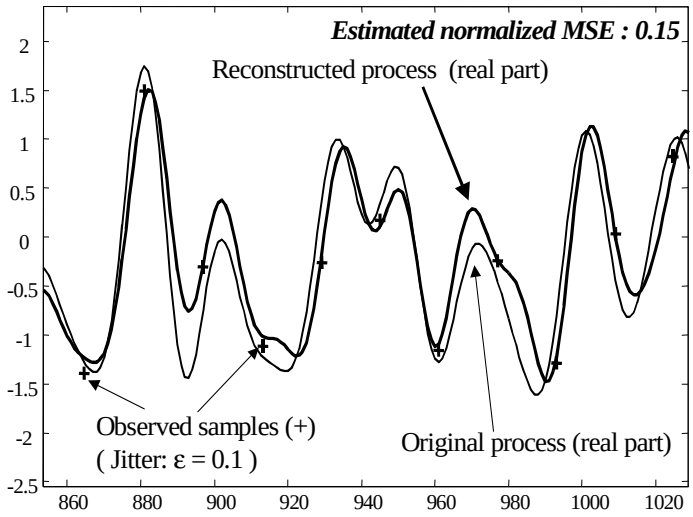


Figure 10: Example of a complex random process (only the real part is represented) and its reconstruction for $\varepsilon = 0.1$.

expression of these interpolation coefficients is derived. Simulation results illustrate the performance of the proposed interpolator which can be implemented easily as a sum of FIR filters of small order. These simulations are conducted for two particular examples: (1) $Z(t)$ has uncorrelated real and imaginary parts and satisfies the Nyquist conditions and (2) $Z(t)$ has correlated real and imaginary parts and does not satisfy the Nyquist conditions. The performance of the LMMSE is studied in both cases.

This paper provides an interesting reconstruction procedure for complex random processes sampled irregularly. The proposed solution requires the knowledge of spectral informations of the original continuous-time process as well as appropriate jitter characteristic functions. This should not be a problem in most applications. As an example, in telecommunications, the transmitted signals are known (NRZ, RZ, Biphase, ...) and as a consequence, have known PSDs [20].

## References


[1] B. Lacaze, Periodic bi-sampling of stationary processes, *Signal Processing*, **68**, 283-293, 1998.

[2] B. Lacaze, Improving the Nyquist rate for complex stationary process sampling, *Sampling Theory in Signal and Image Processing*, **1**, no.1, 33-52, 2002.

[3] A. V. Balakrishnan, On the Problem of Time Jitter in Sampling, *IEEE Trans. Inform. Theory*, **8**, 226-236,1962.

[4] H. Akaike, Effect of timing-error on the power spectrum of sampled data, *Ann. Inst. Statist. Math.*, **11**, no.3, 145-165, 1960.

[5] T. M. Souders, D. R. Flach, C. Hagwood and G. L. Yang, The effects of timing jitter in sampling systems, *IEEE Trans. Instrum. Meas.*, **39**, no.1, 80-85, 1990.

[6] G. Tong and T. M. Souders, Compensation of Markov estimator error in Time-jittered sampling of nonmonotonic signals, *IEEE Trans. Instrum. Meas.*, **42**, no.5, 931-935, 1993.

[7] D. Mirri, G. Iuculano, G. Pasini and F. Filicori, The Effect of Time-jitter in equispaced sampling wattmeters, *IEEE Trans. Instrum. Meas.*, **47**, no.3, 720-727, 1998.

[8] G. Vandersteen and R. Pintelon, Maximum likelihood estimator for jitter noise models, *IEEE Trans. Instrum. Meas.*, **49**, no.6, 1282-1284, 2000.

[9] I. Sharfer and H. Messer, The Bispectrum of sampled data: Part I- Detection of sampling jitter, *IEEE Trans. Signal Processing*, **41**, no.1, 296-312, 1993.

[10] I. Sharfer and H. Messer, The Bispectrum of sampled data: Part II-Monte-Carlo simulations of detection and estimation of the sampling jitter, *IEEE Trans. Signal Processing*, **42**, no.10, 2706-2714, 1994.

[11] P. Marziliano and M. Vetterli, Reconstruction of irregularly sampled discrete-time bandlimited signals with unknown sampling locations, *IEEE Trans. Signal Processing*, **48**, no.12, 3462-3471, 2000.

[12] A. Jerri, The Shannon sampling theorem - Its various extensions and applications: a tutorial review, *Proc. IEEE*, **65**, no.11, 1565-1596, 1977.

[13] A.M. Yaglom, *Theory of random functions*, Prentice Hall, 1962.

[14] B. Lacaze, *Processus Aléatoires pour les communications numériques*, Hermes, 2000.

[15] E. Lukacs, *Characteristic functions*, London: Griffin, 3rd ed., 1970.

[16] B. Lacaze, Stationary clock changes on stationary processes, *Signal Processing*, **55**, no.2, 191-205, 1996.

[17] B. Lacaze, A note about stationary random process sampling, *Stat. Prob. Lett.*, **31**, 133-137, 1996.

[18] A. Papoulis, *Probability, random variables and stochastic processes*, New-York: McGraw-Hill, 1965.

[19] J.G. Proakis, C.M. Rader, F. Ling, and C.L. Nikias, *Advanced digital signal processing*, Macmillan Publishing Company, 1992.

[20] J.G. Proakis, *Digital communications*, New-York: McGraw-Hill, 1995.

[21] H. Cramer and M. R. Leadbetter, *Stationary and related stochastic processes*, New York: Wiley, 1967.

## Appendix A: Time-invariant filter

The time-invariant filter $\mathcal{G}$ of impulse response $g(t)$ associates the stationary process $\mathbf{V} = \{V(t), t \in \mathbb{R}\}$ to the process $\mathbf{W} = \mathcal{G}[\mathbf{V}] = \{W(t), t \in \mathbb{R}\}$ by the relation (defined in some sense)

$$W(t) = \mathcal{G}[\mathbf{V}](t) = \int_{-\infty}^{+\infty} g(t-u) V(u) du. \tag{36}$$

The transfer function of $\mathcal{G}$ is the function $G(\omega)$ defined by

$$G(\omega) = \int_{-\infty}^{+\infty} g(u) e^{-i\omega u} du. \tag{37}$$

Let $H_V$ denotes the Hilbert space spanned by the random process $\mathbf{V} = \{V(t), t \in \mathbb{R}\}$ where the inner product is defined by

$$\langle V(t_1), V(t_2) \rangle_{H_V} = E[V(t_1) V^*(t_2)]. \tag{38}$$

In what follows, an isometry $I_V$, between $H_V$ and $L^2(s_V)$, is defined by the one-to-one correspondence

$$V(t) \overset{I_V}{\longleftrightarrow} e^{i\omega t}, \tag{39}$$

the inner product in $L^2(s_V)$ being

$$\langle f, g \rangle_{L^2(s_V)} = \int_{\mathbb{R}} f(\omega) g^*(\omega) s_V(\omega) d\omega. \tag{40}$$

Consequently, every random variable $A$ (resp. $B$) in $H_V$ will have a corresponding element $f(\omega)$ (resp. $g(\omega)$) in $L^2(s_V)$ such that

$$A = \lim_{n \to \infty} \sum_{k=-n}^{n} a_{kn} V(t_{kn}) \overset{I_V}{\longleftrightarrow} f(\omega) = \lim_{n \to \infty} \sum_{k=-n}^{n} a_{kn} e^{i\omega t_{kn}} \tag{41}$$

and

$$\langle A, B \rangle_{H_V} = E[AB^*] = \int_{\mathbb{R}} f(\omega) g^*(\omega) s_V(\omega) d\omega = \langle f, g \rangle_{L^2(s_V)}. \tag{42}$$

This "fundamental isometry" [21] in the case of the time-invariant linear filter $\mathcal{G}$ defined in (36) and (37) leads to

$$\begin{cases} V(t) \overset{I_V}{\longleftrightarrow} e^{i\omega t} \\ \mathcal{G}[\mathbf{V}](t) \overset{I_V}{\longleftrightarrow} G(\omega) e^{i\omega t}. \end{cases} \tag{43}$$

# Appendix B: LMMSE derivation

The linear minimum mean square estimator (LMMSE) of $W(n)$ based on the observations of $U(n)$ and $V(n)$ is defined by the orthogonal projection of $W(n)$ onto the Hilbert space spanned by the random sequences $\mathbf{U} = \{U(n), n \in \mathbb{Z}\}$ and $\mathbf{V} = \{V(n), n \in \mathbb{Z}\}$

$$\widehat{W}(n) = \underset{H(\mathbf{U}) + H(\mathbf{V})}{\Pr} [W(n)]. \tag{44}$$

$H(\mathbf{U})$ and $H(\mathbf{V})$ are Hilbert spaces spanned respectively by $\mathbf{U} = \{U(n), n \in \mathbb{Z}\}$ and $\mathbf{V} = \{V(n), n \in \mathbb{Z}\}$. Both spaces are generally not orthogonal. Consequently, the sum $H(\mathbf{U}) + H(\mathbf{V})$ can be written in the following manner:

$$H(\mathbf{U}) + H(\mathbf{V}) = H(\mathbf{U}) \oplus H(\mathbf{B}) \tag{45}$$

where $\oplus$ denotes an orthogonal sum and the random sequence $\mathbf{B} = \{B(n), n \in \mathbb{Z}\}$ is defined as a linear function of both observed random sequences $\mathbf{U}$ and $\mathbf{V}$ such that

$$E[U(n)B^*(n-m)] = 0 \qquad \forall (n,m) \in \mathbb{Z}^2. \tag{46}$$

Consequently, the expression of $\widehat{W}(n)$ is derived in four steps:

**Step 1 :** determination of the random sequence $\mathbf{B}$ using (46),

**Step 2 :** orthogonal projection of $W(n)$ onto the Hilbert space $H(\mathbf{U})$,

**Step 3 :** orthogonal projection of $W(n)$ onto the Hilbert space $H(\mathbf{B})$,

**Step 4 :** construction of $\widehat{W}(n) = \mathrm{Pr}_{H(\mathbf{U})}[W(n)] + \mathrm{Pr}_{H(\mathbf{B})}[W(n)]$.

The final step for the LMMSE derivation consists of computing MSE which provides an appropriate performance measure.

These steps are detailed in what follows.

### Step 1

The random sequence $\mathbf{B}$ defined by (46) is chosen to be of the form

$$B(n) = V(n) - \mathcal{H}_B[U](n) \tag{47}$$

where $\mathcal{H}_B[U](n)$ denotes the output of a linear filter driven by $U(n)$. The transfer function of this filter is denoted $H_B(\omega)$ in what follows.

Using the stationary intercorrelation property of $\mathbf{U}$ and $\mathbf{V}$ and the above expression of $B(n)$, (46) can be written

$$\int_{-\pi}^{+\pi} \widetilde{s}_{UV}(\omega)\, e^{i\omega m} d\omega - \int_{-\pi}^{+\pi} H_B^*(\omega)\, e^{i\omega m} \widetilde{s}_U(\omega)\, d\omega = 0 \qquad \forall m \in \mathbb{Z}. \tag{48}$$

The unicity of Fourier transforms leads to the expression of the following filter transfer function:

$$H_B(\omega) = \frac{\widetilde{s}^*_{UV}(\omega)}{\widetilde{s}_U(\omega)}. \tag{49}$$

The PSD of $B(n)$ is then obtained by Wiener-Lee relation [19]

$$\widetilde{s}_B(\omega) = \widetilde{s}_V(\omega) - \frac{|\widetilde{s}_{UV}(\omega)|^2}{\widetilde{s}_U(\omega)}. \tag{50}$$

**Step 2**

The orthogonal projection $W_U(n)$ of $W(n)$ onto the Hilbert space $H(\mathbf{U})$ can be found using the isometry $I_U$ (see previous Appendix A for recalls on isometry). Denote as

$$\begin{aligned} U(n) &\xleftrightarrow{I_U} e^{i\omega n} \\ W_U(n) &\xleftrightarrow{I_U} H_{UW}(\omega)\, e^{i\omega n}. \end{aligned} \tag{51}$$

The orthogonal projection $W_U(n)$ is defined by

$$E\left[\left(W(n) - W_U(n)\right) U^*(n-m)\right] = 0 \qquad \forall (n,m) \in \mathbb{Z}^2. \tag{52}$$

or equivalently

$$\int_{-\pi}^{+\pi} \widetilde{s}_{WU}(\omega)\, e^{i\omega m} d\omega - \int_{-\pi}^{+\pi} H_{UW}(\omega)\, e^{i\omega m} \widetilde{s}_U(\omega)\, d\omega = 0 \qquad \forall m \in \mathbb{Z}. \tag{53}$$

Consequently, $W_U(n)$ can be viewed as the output of a linear filter, driven by $U(n)$, with transfer function

$$H_{UW}(\omega) = \frac{\widetilde{s}_{WU}(\omega)}{\widetilde{s}_U(\omega)}. \tag{54}$$

**Step 3**

The orthogonal projection $W_B(n)$ of $W(n)$ onto the Hilbert space $H(\mathbf{B})$ can be found using the isometry $I_B$ (see Appendix A). Denote as

$$\begin{aligned} B(n) &\xleftrightarrow{I_B} e^{i\omega n} \\ W_B(n) &\xleftrightarrow{I_B} H_{BW}(\omega)\, e^{i\omega n}. \end{aligned} \tag{55}$$

The orthogonal projection $W_B(n)$ is defined by

$$E\left[\left(W(n) - W_B(n)\right) B^*(n-m)\right] = 0 \qquad \forall (n,m) \in \mathbb{Z}^2. \tag{56}$$

or equivalently, $\forall m \in \mathbb{Z}$

$$\int_{-\pi}^{+\pi} \left(\widetilde{s}_{WV}(\omega) - H_B^*(\omega)\,\widetilde{s}_{WU}(\omega)\right) e^{i\omega m} d\omega - \int_{-\pi}^{+\pi} H_{BW}(\omega)\, e^{i\omega m} \widetilde{s}_B(\omega)\, d\omega = 0. \tag{57}$$

By using (49) and (50), $W_B(n)$ can be viewed as the output of a linear filter driven by $B(n)$ with transfer function

$$H_{BW}(\omega) = \frac{\widetilde{s}_{WV}(\omega)\,\widetilde{s}_U(\omega) - \widetilde{s}_{WU}(\omega)\,\widetilde{s}_{UV}(\omega)}{\widetilde{s}_U(\omega)\,\widetilde{s}_V(\omega) - |\widetilde{s}_{UV}(\omega)|^2}. \tag{58}$$

**Step 4**

Up to this point, it has been shown that the LMMSE $\widehat{W}(n)$ of $W(n)$ can be defined by linear filtering of $U(n)$ and $V(n)$ as illustrated in Fig. 11.

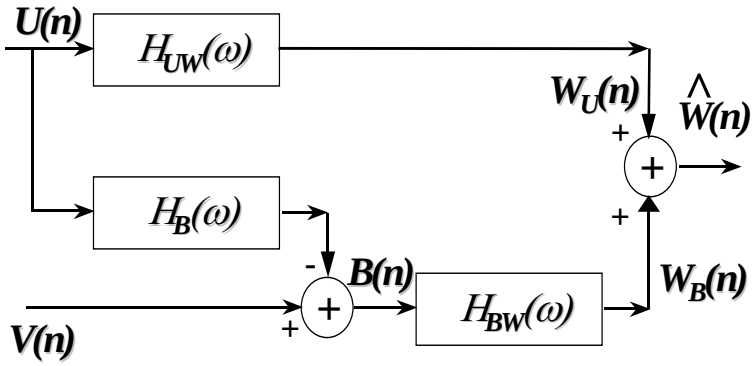


Figure 11: Detailed scheme of reconstruction of $W(n)$ from the observation of $U(n)$ and $V(n)$.

This procedure is equivalent to the Fig. 1 where

$$\begin{aligned} H_U(\omega) &= H_{UW}(\omega) - H_B(\omega)\, H_{BW}(\omega) \\ H_V(\omega) &= H_{BW}(\omega). \end{aligned} \tag{59}$$

Note that in the particular case $\mathbf{W} = \mathbf{U}$, we obtain $H_V(\omega) = 0$ and $H_U(\omega) = 1$ (the same holds if $\mathbf{W} = \mathbf{V}$).

**MSE**

The MSE between $W(n)$ and $\widehat{W}(n)$ is defined by

$$\begin{aligned}\sigma_W^2 &= E\left[\left|W(n) - \widehat{W}(n)\right|^2\right] = E\left[\left(W(n) - W_U(n) - W_B(n)\right) W^*(n)\right] \\ &= K_W(0) - \int_{-\pi}^{+\pi} H_{UW}(\omega)\, \widetilde{s}_{UW}(\omega)\, d\omega \\ &\quad - \int_{-\pi}^{+\pi} H_{BW}(\omega)\left(\widetilde{s}_{VW}(\omega) - H_B(\omega)\, \widetilde{s}_{UW}(\omega)\right) d\omega. \end{aligned} \tag{60}$$

Equations (49), (54) and (58) yield

$$\sigma_W^2 = K_W(0) - \int_{-\pi}^{+\pi} \Delta(\omega)\, d\omega \tag{61}$$

where

$$\Delta(\omega) = \frac{\left|\widetilde{s}_{WU}(\omega)\right|^2}{\widetilde{s}_U(\omega)} + \frac{\left|\widetilde{s}_{WV}(\omega)\, \widetilde{s}_U(\omega) - \widetilde{s}_{WU}(\omega)\, \widetilde{s}_{UV}(\omega)\right|^2}{\widetilde{s}_U(\omega)\left(\widetilde{s}_U(\omega)\, \widetilde{s}_V(\omega) - \left|\widetilde{s}_{UV}(\omega)\right|^2\right)}. \tag{62}$$

Note that in the particular case $\mathbf{W} = \mathbf{U}$, $\Delta(\omega) = \widetilde{s}_U(\omega)$ and $\sigma_n^2 = 0$ (the same holds if $\mathbf{W} = \mathbf{V}$).

## Appendix C: Spectra and interspectra

This section derives the spectra and interspectra $\widetilde{s}_U(\omega), \widetilde{s}_V(\omega), \widetilde{s}_{UV}(\omega), \widetilde{s}_{WU}(\omega), \widetilde{s}_{WV}(\omega)$, which are necessary to derive the LMMSE according to (15). Denote as

$$\begin{aligned} W(n) &= Z(t+n) = X(t+n) + iY(t+n) \\ U(n) &= X(n - A(n)) = \breve{X}(n) \\ V(n) &= Y(n - A(n)) = \breve{Y}(n). \end{aligned}$$

The PSD $\widetilde{s}_U(\omega)$ of $U(n)$ is related to its correlation function by (13). Moreover, conditional expectations yield

$$\begin{aligned}
&E[U(n)U^*(n-m)] \\
&= E\{E[X(n-A(n))X^*(n-m-A(n-m)) \mid \mathbf{A}]\} \\
&= E[K_X(A(n-m)-A(n))] \\
&= E\left[\int_{\mathbb{R}} e^{i\omega(A(n-m)-A(n)+m)} s_X(\omega)\, d\omega\right] \\
&= \int_{\mathbb{R}} \Phi^*(m,\omega)\, e^{i\omega m} s_X(\omega)\, d\omega. \qquad (63)
\end{aligned}$$

Eq. (63) and (13) allow to define $\widetilde{s}_U(\omega)$ as follows

$$\begin{aligned}
\int_{-\pi}^{+\pi} \widetilde{s}_U(\omega)\, e^{i\omega m} d\omega = \sum_{k\in\mathbb{Z}} \int_{-\pi}^{+\pi} \Phi^*(m,\omega+2\pi k)\, e^{i\omega m} s_X(\omega+2\pi k)\, d\omega \\
\forall m \in \mathbb{Z}. \qquad (64)
\end{aligned}$$

The same properties hold for $\widetilde{s}_V(\omega)$ (replace $s_X$ by $s_Y$ in the above expression) and for the interspectrum $\widetilde{s}_{UV}(\omega)$ (replace $s_X$ by $s_{XY}$ in the above expression). The interspectrum $\widetilde{s}_{WU}(\omega)$ can be derived as follows:

$$\begin{aligned}
&E[W(n)U^*(n-m)] \\
&= E\{E[(X(t+n)+iY(t+n))X^*(n-m-A(n-m)) \mid \mathbf{A}]\} \\
&= E\left[\int_{\mathbb{R}} e^{i\omega(t+m+A(n-m))}\left(s_X(\omega)+is^*_{XY}(\omega)\right) d\omega\right] \\
&= \int_{\mathbb{R}} \Psi(\omega)\, e^{i\omega m} e^{i\omega t}\left(s_X(\omega)+is^*_{XY}(\omega)\right) d\omega. \qquad (65)
\end{aligned}$$

By using

$$E[W(n)U^*(n-m)] = \int_{-\pi}^{+\pi} \widetilde{s}_{WU}(\omega)\, e^{i\omega m} d\omega$$

the interspectrum can be expressed as follows:

$$\widetilde{s}_{WU}(\omega) = e^{i\omega t} \sum_{k\in\mathbb{Z}} \Psi(\omega+2\pi k)\, e^{i2\pi kt}\left(s_X(\omega+2\pi k)+is^*_{XY}(\omega+2\pi k)\right). \qquad (66)$$

The same ideas can be used to derive the interspectrum $\widetilde{s}_{WV}(\omega)$ (replace $s_X$ by $s_{XY}$ and $s^*_{XY}$ by $s_Y$ in the above expression). The knowledge of $\widetilde{s}_U(\omega), \widetilde{s}_V(\omega), \widetilde{s}_{UV}(\omega), \widetilde{s}_{WU}(\omega), \widetilde{s}_{WV}(\omega)$ allows to derive the expression of the reconstruction filters $H_U(\omega)$ and $H_V(\omega)$ defined in (59).